ASEAN Journal of Chemical Engineering 2022, Vol. 22, No. 1, 19 – 32

Design, Fabrication, and Testing of Supercapacitor Based on Nanocarbon Composite Material

Heri Rustamaji*[,1,2]
Tirto Prakoso*[,1]
Hary Devianto[1]
Pramujo Widiatmoko[1]
Isdiriayani Nurdin[1]
[1] *Department of Chemical Engineering, Institut Teknologi Bandung, Bandung 40132 Indonesia*
[2] *Department of Chemical Engineering, Lampung University, Bandar Lampung 35145 Indonesia*
*e-mail: heri.rustamaji@eng.unila.ac.id (HR); tirto@che.itb.ac.id (TP)

Submitted 01 November 2021 *Revised* 21 March 2022 *Accepted* 05 April 2022

Abstract. This research investigates the design, fabrication, and testing of single-cell and module supercapacitors. The supercapacitor consists of carbon nanocomposites, which contain activated carbon (AC), multiwall carbon nanotubes (MWCNT), and graphene (GR). The coin and pouch cell type supercapacitors were manufactured with AC: MWCNT: GR composite electrodes in a ratio of 70:20:10 weight percent. Meanwhile, the electrochemical characterization showed that the highest capacitance values for single coin and pouch cells were 32.13 F g^{-1} and 5.3 F g^{-1}, respectively, in 6 M KOH electrolyte at a scan rate of 2 mV s^{-1}. Furthermore, the power and energy densities for the coin-cell supercapacitor were 69 W kg^{-1} and 6.6 Wh kg^{-1}, respectively, while for the pouch cell, it was 7.4 W kg^{-1} and 1.0 Wh kg^{-1}, respectively. The coin-cell supercapacitor durability test was carried out for 1000 cycles, yielding the retention capacitance and coulombic efficiency values of 94-97% and 100%, respectively. These results showed that the performance of the supercapacitor is close to commercial products.

Keywords: Supercapacitor, Nanocarbon, Electrode, Electrochemical, Performance Test

INTRODUCTION

In today's energy-dependent world, electrochemical energy storage systems are essential to deal with the rapidly diminishing supply of fossil fuels (Wang et al. 2017, Simon and Gogotsi 2020). Therefore, the development of supercapacitors has attracted interest in local educational areas and mechanical design in the past few decades due to their beneficial force thickness, quick charge/release rates, and positive life cycles (Agustyn et al. 2014, Bonaccorso et al. 2015, Lukatskaya et al. 2016, Wang et al. 2016).

A supercapacitor is typically a bridge between a traditional battery and a dielectric capacitor. It is used in various apps, for example, consumer electronics, transportation, grid balancing, and power backup to replace batteries. Furthermore, it is combined with secondary batteries to support the extra power needed in these applications (Scibioh and Viswanathan 2020a). Based on the charge storing mechanism, the supercapacitor is categorized into three, namely (i) electric double-layer capacitors (EDLCs), (ii) redox capacitors, and

DOI: 10.22146/ajche.70139

(iii) hybrid capacitors. Supercapacitors are not the same as ordinary capacitors regarding their energy storage or charge, which is withdrawn electrostatically by substance responses between the cathodes of the capacitor and the electrolyte. Although no electrolyte is used for dielectric capacitors, it is used between the two cathodes in the supercapacitor (Cheng et al. 2020)

The primary components of a supercapacitor consist of electrodes, electrolyte, separator, and current collector. Also, carbonaceous materials comprised of activated carbon, carbon aerogel, carbon nanotubes (CNTs), graphene, and carbon nanofibers are frequently used as active components in double-layer electrodes. Meanwhile, due to the excellent surface area, low cost, and ability to be prepared from various precursor sources, activated carbons are still used as a material for practical applications (Azais et al. 2017). However, it is generally assumed that pore volume and measures that oblige solvated particles increase the capacitance esteems. Studies have also shown that frameworks with pore sizes (< 2 nm) fit materials with high capacitance, indicating that some sort of desolvation at the atomic level grants particle transport and adsorption in the micropores.

The method for energy storing carbonaceous material is by creating an electrochemical double layer at the electrode-electrolyte interface. Specific surface area, pore-size distribution, pore shape and structure, electrical conductivity, and surface functioning are the primary parameters impacting their electrochemical performance (Singh et al. 2015, Yang et al. 2017, Antonietti et al. 2018). Meanwhile, the two most essential aspects determining the performance are specific surface area and pore-size distribution. This is because capacitance is primarily determined by the surface area accessible to the electrolyte ions. Similarly, a large specific surface area also increases the ability of a carbonaceous material to accumulate charge at the electrode-electrolyte contact (Scibioh and Viswanathan 2020b). Carbon nanocomposites have been examined to improve supercapacitors' performance by exploiting the synergy properties between activated carbon and other nanocarbon materials. Nanocomposites can be a combination of binary, ternary, and quaternary carbon nanomaterials (Kumar et al. 2016). There was no information on composite electrode materials from a variety of activated carbon, CNT, and graphene in this research.

There is a need to develop acceptable electrolytes, electrode materials, current collectors, binder, and solvent with good performance characteristics and low cost for the supercapacitors to have a wide range of applications (Chernysh et al. 2019).

Binders are used to fabricate electrode coating consisting of active ingredient material such as nanocarbon, which retains the physical stability of the layer and ensures a strong bond between the energetic particles and the current collector. The compatibility of the binder with the solvent will affect the quality of the electrode coating on the current collector. Both also affect the wettability of the electrode to the electrolyte. Different electrolytes have different ionic conductivity and potential windows. Interactions between electrolytes with active and inactive materials such as solvent binders and current collectors affect the performance and reliability of supercapacitors (Zhong et al. 2015).

Therefore, this research aims to determine the performance of supercapacitors with electrodes from nanocarbon composites, which consist of activated carbon, CNT, and graphene. Furthermore, the impact of electrodes, electrolytes, binders, and solvents on the supercapacitor's performance was evaluated. The coin and pouch cell supercapacitors were also characterized by potentiostats.

In this study, the use of a deep eutectic solvent of ChCl was introduced as a new ionic electrolyte in addition to the aqueous electrolyte KOH. The results showed that PVDF and ethanol solvents for coating electrodes on current aluminum collectors have good adhesive properties and are suitable for using ChCl electrolyte with the highest capacitance among other samples. However, the cell stability of this combination is not good because of the volatile ethanol solvent, so the electrodes quickly fade from the current collector. CMC binder and water solvent combined with KOH electrolyte become excellent and stable for practical application.

MATERIAL AND METHODS

Material

In this research, activated carbon (AC), multiwall carbon nanotube (MWCNT), and graphene (GR) multilayer were used to make the composite electrode material. The commercial AC was purchased from CV. EstraChemical (Tangerang, Indonesia) consisted of a nominal BET (Brunauer, Emmett, and Teller) surface area of 832.9 m^2 g^{-1} and a diameter pore size of 4.05 nm. Furthermore, XFNano supplied industrial quality MWCNT with outer and inner diameters, tube lengths, specific surface areas, apparent density, and conductivity of 50 nm, 5-15 nm, 10-20 m, 60 m^2 g^{-1}, 0.19 g cm^{-3}, and 100 S m^{-1}, respectively (Jiangsu, China). Industrial-grade graphene nanoparticles are used with a specific surface area, apparent density, and conductivity of 31.657 m^2 g^{-1}, 0.09-0.10 g cm^{-3}, and 550-1000 S m^{-1}, respectively, potassium hydroxide (KOH, Merck, 99%), ethylene glycol ($C_2H_6O_2$, Merck, 99%), and ethanol (C_2H_5OH, AR, 96%), carboxymethylcellulose (CMC, 60%), and polyvinylidene fluoride (PVDF, 65%) were purchased from PT. Bratachem, Bandung. Choline chloride powder (ChCl, 99%) for electrolyte was purchased from Salus Nutra Inc., Xian, China.

Nanocomposite Preparation

The composite electrode material consisted of AC, MWCNT, and GR with a composition of 70:20:10 wt.% and 10 wt.% PVDF of nanocarbon. The powders were dispersed in ethanol and mixed with sonication for 30 min. A mixture of dry electrode materials was used as a supercapacitor coin cell electrode material. The electrode material for the pouch cell was prepared with the same nanocarbon composition. However, PVDF and CMC were used as binders. Subsequently, the mixture of nanocarbon and binder was added with demineralized water three times the total weight of the material and mixed with a ball mill mixing for 3 hours. The electrode material was dried in an oven at 105°C for 24 hours.

Coin and Pouch Cell Supercapacitor Assembly

Coin cell electrode was prepared from 0.2 g of the dry composite mixture, molded, and pressed at 7-10 MPa to obtain a circle electrode with a diameter and thickness of 15 mm and 1 mm, respectively. A coin cell (CR2302) type supercapacitor was manufactured with two electrodes at a mass loading of 2.30 mg cm^{-2}. Furthermore, a

Whatman filter paper was used to separate the two electrodes in 6 M KOH, and the cell was pressed using a hydraulic machine (Liu and Liu 2017).

Pouch cell electrodes were prepared by applying a slurry of the electrode material to the current collector using a doctor blade. The thickness of the coating was set to uniform. The coated current collector was heated at 40°C for 24 hours. The 12 coated current collectors were stacked with filter paper as separator and KOH as electrolyte. Meanwhile, five interfaces of the stacked current collector were wrapped with aluminum laminated polyamide and sealed at a temperature of 180°C (Trask et al. 2014).

Electrochemical Characterization

The electrochemical behavior of samples was characterized using a potentiostat (Gamry V3000). The characterization consists of electrochemical impedance spectroscopy (EIS), galvanostatic charge-discharge (GCD), and cyclic voltammetry (CV) based on a two-electrode system.

The EIS study was carried out over a frequency range of initial and final values of 100 kHz and 1 Hz, respectively. GCD analysis was carried out at a current density of 1 mA cm^{-2}; meanwhile, CV analysis was carried out in the voltage range -0.3 – 0.6 V and scan rate variations (2, 4, 6, 8, and 10 mV s^{-1}). At the same time, the stability test cycle was conducted using a cyclic discharge-charge measurement at a constant current of 50 mA. Eqs. (1) was adopted to determine the specific capacitances of supercapacitors computed from CV curves (Cheng et al. 2011), where C_{spa} denotes the specific capacitance (F g^{-1}), (V_2-V_1), is the voltage sweep range (V), m is the mass of the active electrode (g), and i(V)dt is the area under the CV curve. Meanwhile, energy density, E (Wh kg^{-1}), and power density, P (W kg^{-1}), are calculated from Eqs. (2) and (3), respectively.

$$C_{spa} = \frac{2}{m|V_2 - V_1|}\int_{t=0(V_1)}^{t(V_2)} i(V)dt \quad (1)$$

$$E = \frac{1}{2}C_{spa}V^2 \quad (2)$$

$$P = \frac{E\ x\ 3600}{t_{disch}} \quad (3)$$

Discharge time (second) and operating potential (V) are represented by t_{disch} and V, respectively.

RESULTS AND DISCUSSION

Coin and Pouch Cell Analysis

Figure 1 shows the electrochemical characterization results of the coin cell supercapacitor, while Figure 1a shows a quasi-rectangular coin cell consistently at a scan rate of 2-10 mV s^{-1}. The quasi-rectangular shape of a voltammogram indicates characteristics of the electrical double layer. The profile also shows that the double layer capacitance is formed because the electrolyte ions are adsorbed abundantly on the material's surface with little diffusion resistance in the electrolyte (Liu et al. 2016).

The GCD curve of the coin cell supercapacitor, as shown in Figure 1b, indicates the charge/discharge process with a current density of 1 mA cm^{-2}. Figure 1b offers a relatively good charge/discharge process, as noted in the occurrence of a discharge after 200 seconds. This also occurs when the final and initial voltage are not the same and the triangle formed is not symmetrical. The imperfect discharge process on the GCD curve shows that the ions are not well desorbed at the given current value, or the electrolyte ions are reacting with the electrodes (Balducci et al. 2017).

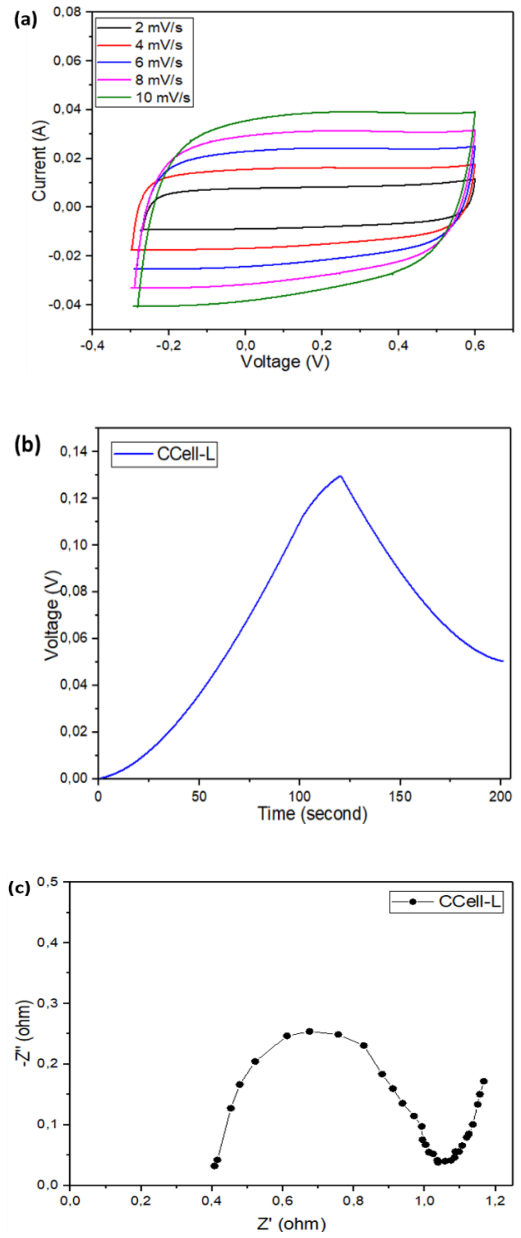

Fig. 1: Electrochemical characterization of Coincell. (a) cyclic voltammetry curve, (b) galvanostatic charge/discharge curve, and (c) electrochemical impedance spectroscopy curve.

Figure 1c shows the EIS curve in a Nyquist plot for a coin cell supercapacitor at a frequency of 1-10^5 Hz. A semicircular graph shows the value contact resistance between the electrode material and the current collector. Meanwhile, the semicircular region of the small value indicates low electrical resistance between the electrodes, good conductance, and the current collector (Beguin and Frackowiak 2013).

Based on the experimental results of the pouch cell, as shown in Table 1, the PC-ACC sample has the highest capacitance. This cell is manufactured from nanocomposite material with PVDF binder and ethanol solvent on a current aluminum collector with ChCl electrolyte. Aluminum is a current collector which has a higher electrical conductivity than stainless steel (σ_{Al} = 35×10^4 S cm^{-1} > σ_{SS} = 1.45 × 10^4 S cm^{-1}) and has a lower resistivity than stainless steel (ρ_{Al} = 2.82×10^{-8} Ω.m < ρ_{SS} = 6.9×10^{-7} Ω.m) (Giurlani et al. 2022).

Meanwhile, PVDF is a homopolymer material with a high dielectric constant and high viscosity and affinity in N−methyl-pyrrolidinone, dimethylsulfoxide, and ethanol solvents (Marshall et al. 2021). Thus, the combination of these materials results in low charge transfer resistance and resistance between the electrodes and the current collector. On the other hand, the electrolyte ChCl in ethylene glycol solution has a lower electrical conductivity than the KOH electrolyte (σ_{ChCl} = 11.75 mS cm^{-1}< σ_{KOH}= 626.6 mS cm^{-1}), but has a higher window potential (V_{ChCl} = 2.2 V > V_{KOH} = 1.2 V) which helps increase the specific capacitance (Allebrod et al. 2012).

Furthermore, the electrochemical characterization for each pouch cell product is shown in Figure 2. Figure 2b shows the cyclic voltammogram of the supercapacitor with variations at the scan rate of 2 mV s^{-1} in the 6 M KOH electrolyte. The cyclic voltammograms of all products are parallelograms, which indicate the typical double-layer electrical supercapacitor (EDLC) behavior, rapid charge/discharge method with high power, and low equivalent series resistance (Cheng et al. 2011).

The GCD curves (Figure 2c) for PC-ACP, PC-SKC, and PC-SCC products show a symmetrical triangle, indicating a low resistance. Meanwhile, the GCD curves for PC-AKP and PC-ACC products show an asymmetrical triangle, which means higher resistance. Figure 2d shows the EIS curves of all pouch cell products with different shapes, and the PC-SCC has a minor semicircle shape among other supercapacitors.

Table 1. Experiments for fabrication of pouch cells and their capacitance value

No.	Product	Current Collector	Electrolyte	Binder/ Solvent	Capacitance ($F\ g^{-1}$)
1	PC-ACC	Aluminum	2.4 M ChCl	CMC/Water	3.13
2	PC-ACP	Aluminum	2.4 M ChCl	PVDF/Ethanol	7.28
3	PC-SKC	Stainless steel sieve	6 M KOH	CMC/Water	2.57
4	PC-AKP	Aluminum	6 M KOH	PVDF/Etanol	5.14
5	PC-SCC	Stainless steel sheet	6 M KOH	CMC/water	5.30

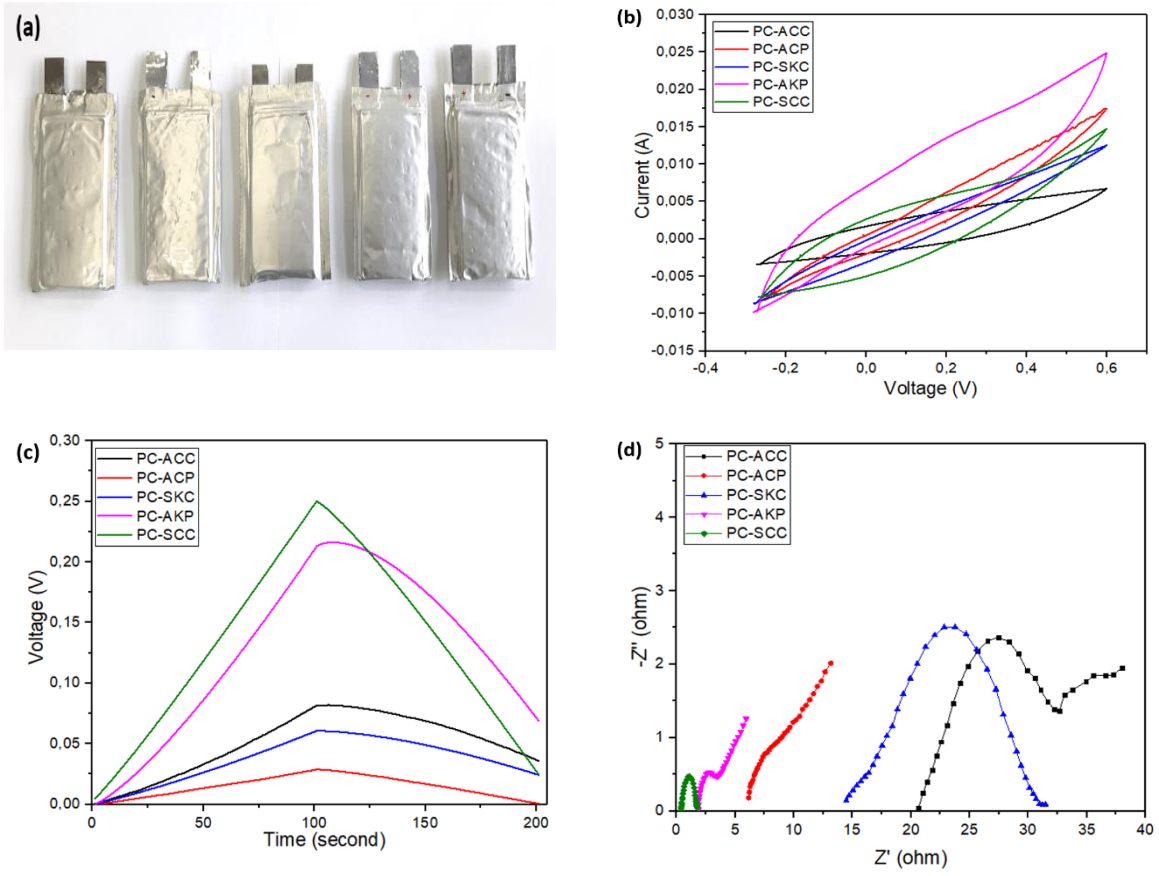

Fig. 2: Pouch cells characterization (a) Pouch cells supercapacitor, (b) Cyclic voltammogram, (c) GCD, and (d) EIS curves for all samples.

In addition, a small semicircle indicates that the internal resistance of the electrode layer and the resistance due to contact with the current collector is small (Yang et al. 2017). Generally, the CV curve correlated with the EIS curve. A supercapacitor with a broad CV curve would have a large specific capacitance when showing an EIS curve with a slight resistance value. In the initial development of supercapacitors, CV results become the basic information about the capacitive properties of an electrochemical cell, the potential window, capacitance, and life cycle. EIS is chosen as the method to measure the equivalent series resistance (ESR) of the supercapacitor. Therefore, when the CV curve does not correlate with the EIS in some cases, it is usually chosen as a reference (Shao et al. 2020).

Re-testing of all samples was carried out in one week to determine the supercapacitor product's stability and showed the readings on the potentiostat become errors for pouch cells with PVDF binder and ethanol solvent. This phenomenon may occur because cell electrodes with PVDF binder and ethanol solvent tend to fade from the current collector quickly. Thus, cell bags with CMC binders and water sailors with KOH electrolytes become more suitable for practical applications.

Specifications of Supercapacitor

Specifications for laboratory and commercial supercapacitors are listed in Table 2. The capacitive value is usually expressed in farads per unit active mass (C_{spa}). Since there are no data on the active material of commercial supercapacitors and only the capacitance value is known, the capacitance is expressed in farads per unit total weight of electrode and casing (C_{spt}). Table 2 showed that the supercapacitors from this research could compete with commercial products.

Electrochemical characterization was carried out on commercial supercapacitor products for cylinder (SC-1) and double coin cell (SC-2). The characterization of the laboratory and commercial supercapacitor is shown in Figure 3. In contrast, the voltammogram curve for each supercapacitor is shown in Figure 3a. Meanwhile, the coin cell voltammogram curve is similar to the nearly rectangular SC-1, indicating good capacitive electric double layer properties. Meanwhile, the voltammogram for pouch cell and SC-2 are in the form of a parallelogram, which means the behavior of the double-layer capacitor (EDLC) type with a fast charge/discharge process, high power, and low equivalent series resistance (Cheng et al. 2011, Liang et al. 2019).

Table 2. Specifications of laboratory and commercial supercapacitor

Product	Type	W_{total} (g)	C_{cell} (F)	C_{spt} (F g^{-1})	E (Wh kg^{-1})	P (W kg^{-1})	I_{max} (A)
SC-1	Cylinder	2.1	6.0	2.85	2.89	3.2	2.3
SC-2	Double coin	9.1	1.0	0.1	0.42	0.25	n.a.
CCell-L (This work)	Coin	3.0	13.2	4.4	0.88	10.90	0.7
Pcell-L (This work)	Pouch	23	20	0.87	0.17	1.28	0.9

SC-1/2/3/4: Commercial supercapacitor of 1/2/3/4, W_{total}: total weight of electrode and casing, CCell-L: Coin cell laboratory (C_{spa}: 32.13 F g^{-1}), PCell-L: Pouch cell laboratory (C_{spa}: 5.3 F g^{-1}), C_{cell}: Capacitance of cell, C_{spt}: Capacitance per total weight, E: energy density, P: power density, I_{max}: maximum current,

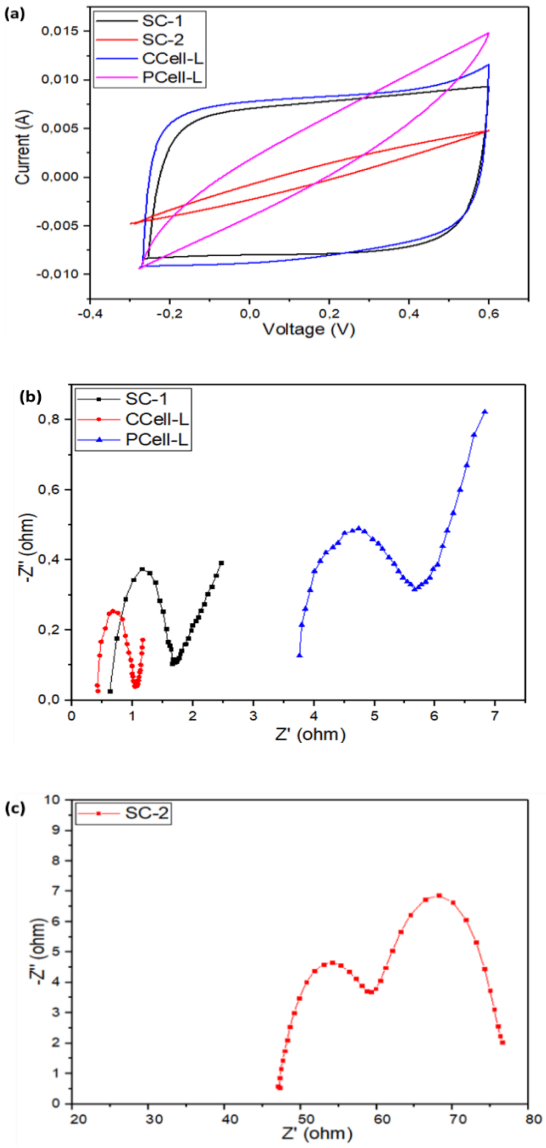

Fig. 3: (a) Voltammogram curves of SC-1, SC-2, CCell-L, and PCell-L, (b) Nyquist curves of three supercapacitors, and (d) Nyquist curve for SC-2.

Based on Figure 3b, the EIS curve is a Nyquist plot for the SC-1, CCell-L, and PCell-L, while the semicircular area shows the contact resistance between the current collector and the electrode material.

The semicircular region of the small value also indicates low electrical resistance between the electrodes, good conductance, and the current collector. Furthermore, it shows that the coin cell has the smallest semicircular area between the SC-1 and PCell-L. Meanwhile, Figure 3c illustrates a Nyquist curve plot with two semicircular figures with large values, which indicates an extended diffusion limit at the supercapacitor electrode (Zheng and Gao 2011).

Figure 4 shows the GCD curve for each supercapacitor. The curve of SC-1 and CCell-L in Figures 4a and 4c indicates an imperfect charge/discharge process because there is no voltage discharge after 100 seconds. The absence of a voltage drop on the curve shows that the ions are not well desorbed at the given current value, or the electrolyte ions react with the electrodes (Sinha et al. 2020). Meanwhile, the GCD curve for SC-2 and coin cell in Figure 4b shows a good charge/discharge process characterized by a decrease in voltage after 100 seconds, although the triangle formed is not symmetrical. Figure 4d shows a perfect charge/discharge process by creating a symmetrical triangle. Therefore, laboratory supercapacitor has good character and can compete with commercial products.

A durability test was conducted by cyclic charge-discharge (CCD) analysis using a potentiostat to determine the life cycle of supercapacitor products. At a specific voltage and current and the desired cycle, the charge/discharge character of the supercapacitor in the multicycle was obtained.

The cycle life of the supercapacitor is determined by examining the coulomb efficiency (CE) and capacitance retention (CR). Moreover, CE is the discharge capacity ratio to the charge capacity in a given cycle. At the same time, CR is the ratio between the capacitance of each process to the initial

capacitance. When the CE value in 1000 cycles is still stable above 90%, it is estimated that the supercapacitor's life is extended (Zhang et al. 2013). Meanwhile, Balducci et al. (2017) recommend a CCD test of 10,000 cycles to measure and predict the lifetime of the supercapacitor. Based on the test, CCD measurement at 1000 cycles showed that the supercapacitor has a relatively constant CE at 100%. Meanwhile, the CR value at 1000 cycles indicated a relatively stable value at 96%, as shown in Figure 5.

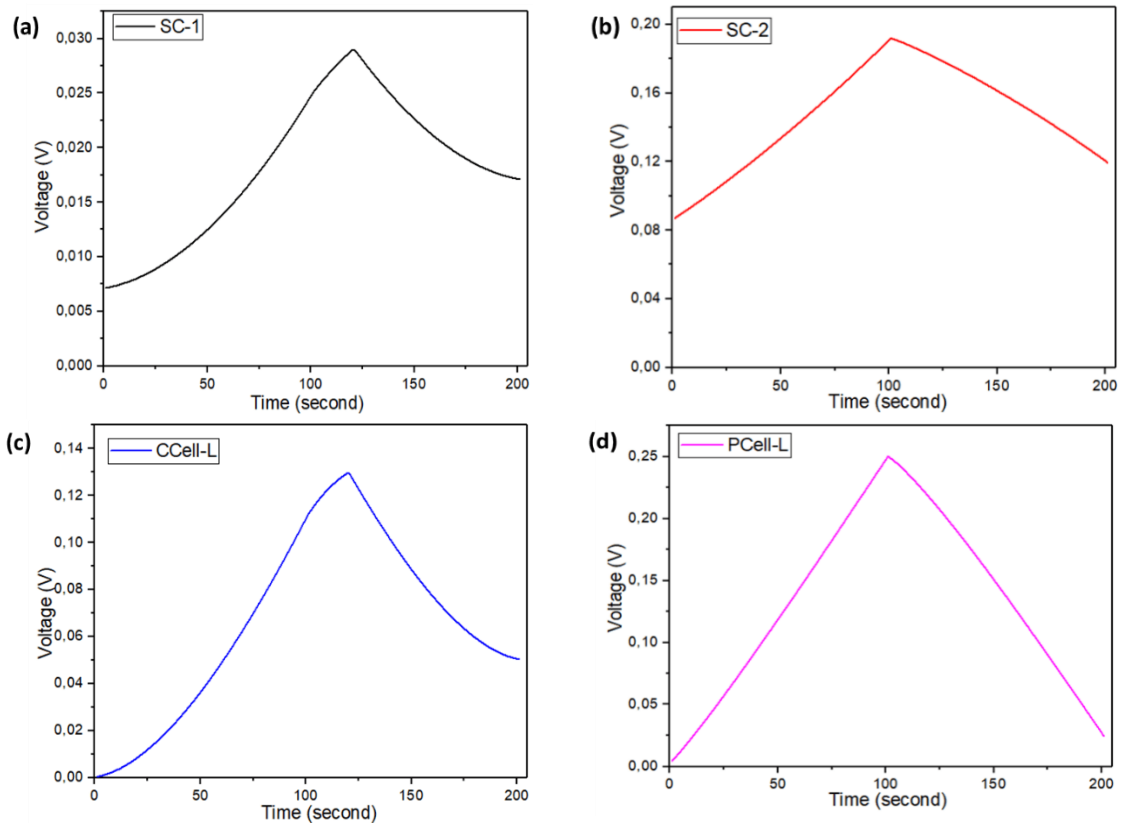

Fig. 4: GCD curve of supercapacitor at 1 mA cm^{-2}. (a) SC-1, (b) SC-2, (c) CCell-L, and (d) PCell-L.

Figure 5a represents the CE and CR curves for the SC-1 for 1000 cycles, showing that the CE value in the first ten cycles is 88-98%, and it increases to 100% until the cycle is 1000 (red line). This indicates that the supercapacitor passes through a relatively rapid stabilization process in the initial ten cycles and is constant until the 1000th cycle. Moreover, the CR value changed from the first ten cycles and stabilized at 94% until the last cycle. The inset image shows the GCD curve of SC-1 for ten processes with stable values. Based on Figure 5b, the CE and CR curves for the CCell-L for 1000 cycles, the CE value in the first 300 cycles was 101%, decreased to 100% until the cycles reached 1000 (red line).

The phenomenon indicates that the supercapacitor passes through a stabilization process in the first 300 cycles and is constant until the 1000th cycle. This process is influenced by the transfer of electrolyte ions in the electrodes. The CR value changed from the first 300 cycles and stabilized at a level of

97% until the cycle was 1000. Moreover, the inset image shows the coin cell's GCD curve for ten relatively consistent processes.

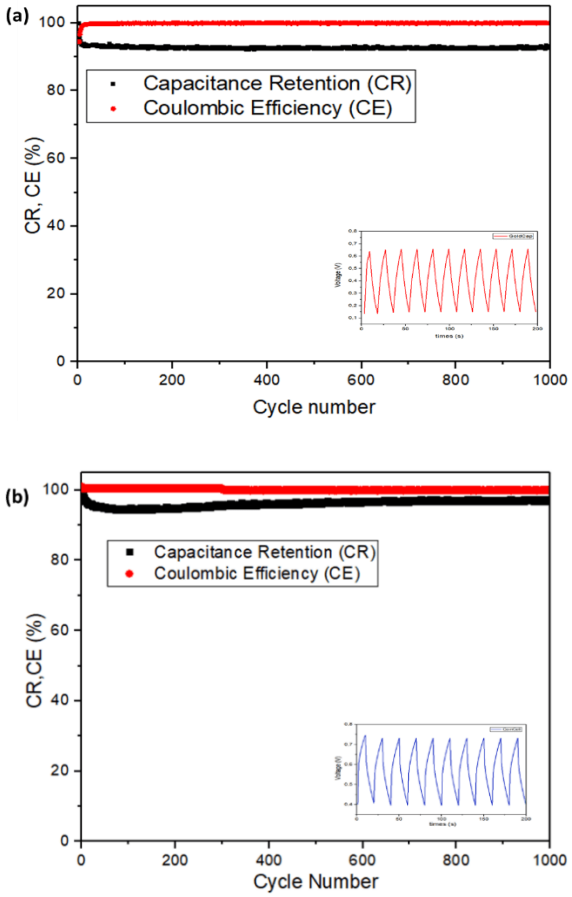

Fig.5: Coulombic efficiency and capacitance retention curve of supercapacitor. (a) SC-1 and (b) CCell-L.

Table 3 compares supercapacitors synthesized from carbon material and nanocomposites with a two-electrode system. Based on this table, the cell capacitance in this study was higher than in other studies using organic electrolytes (Et_4NBF_4) because the ion conductivity of the KOH electrolyte is higher so that the ion mobility is faster, lowering the series equivalent resistance and providing increased power. Meanwhile, compared to the research of Yang et al. (2018) and Wulandari et al. (2021), which used the same electrolyte, the cell capacitance of this study was higher, indicating that the conductivity of the nanocomposite electrode material was higher.

On the other hand, the capacitance of this study is lower than Xu et al. (2018) and Liu et al. (2018), presumably due to the influence of the rich nitrogen and phosphorus content of the biomass used (natural casing and soybean pods). A high nitrogen content increases the wettability of the electrode to the electrolyte, lowers the resistance between the electrode phases, and provides a redox effect, thereby increasing the capacitance (Pal et al. 2021).

Table 3. Comparison of electrochemical performance of various carbon materials with nanocarbon composite

Material	Electrolyte	C_{spa} (F g^{-1})	E (Wh kg^{-1})	P (W kg^{-1})	Reference
Petroleum activated carbon	1 M Et_4NBF_4	29.6	n.a.	n.a.	Stephane et al. 2021
Biomass activated carbon	6 M KOH	25.7	n.a.	n.a.	Yang et al. 2018
Biomass activated carbon	6 M KOH	42.6	11.6	298	Xu et al. 2013
Biomass activated carbon	1 M Na_2SO_4	40.1	22.3	450	Liu et al. 2018
Biomass activated carbon	6 M KOH	29.5	n.a.	n.a.	Wulandari et al. 2021
Nanocarbon composite	6 M KOH	32.1	6.60	69	This work

Testing Supercapacitor Module

Some coin cell supercapacitors were arranged in series and parallel in one module to meet electronic devices' voltage and current requirements. The charged cells were used to power mini dynamos. Meanwhile, to

drive a mini dynamo motor (3.2 V, 0.7 A), eight supercapacitor coin cells with a four series circuit and two parallel (4S2P) are required.

Table 4. Specification of coin cell-based packed module

No	Parameter	Value
1	Nominal voltage, V	3.2
2	Maximum Voltage, V	3.8
3	Minimum Voltage, V	2.7
4	Capacitance, F	22
5	Spesific Energy, Wh kg^{-1}	44
6	Spesific power, W kg^{-1}	5
7	Discharging Current, A	0.7
8	Charging Current, A	0.9

The module design focused on the mechanical design, module assembly, the active element of the cell, and determination of its shape. This supercapacitor module contains several components, namely a unit cell, a connection between cells and a plate, two electrical terminals, and a polymer-based casing (Beguin and Frackowiak 2013, Tanwilaisiri et al. 2018, Shao et al. 2020). The capacitance, current, and voltage value for a single coin cell supercapacitor cell is 11 F, 0.2 A, and 0.8 Volts. Since the specifications for the module is 22 F, 1.0 A, and 3.2 V, the cell specifications and inputs are defined as shown in Table 4.

Figure 6a shows the outcomes of 3D printing and a series of connectors in the module settings. The entire module, consisting of four series and eight parallel circuits, is charged and tested to drive a 0.7 a mini dynamo motor at 3.2 V, as shown in Figure 6b. The tests showed that coin cells, pouch cells, and coin cell-based supercapacitor modules work magnificently as energy storage and can be used to power electronic devices.

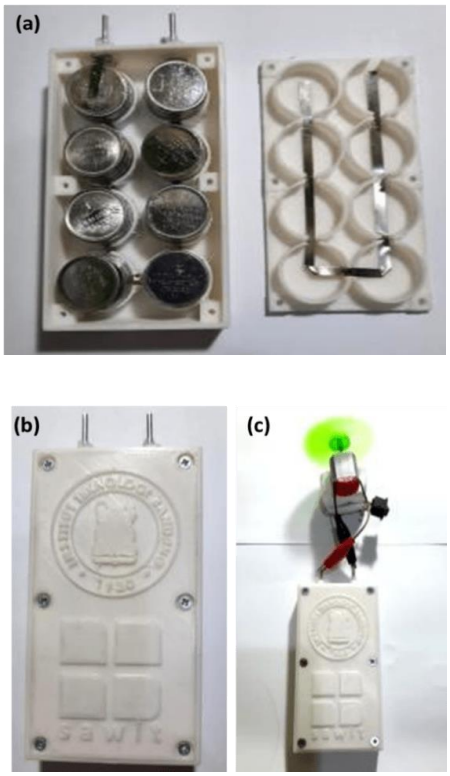

Fig. 6: Coin cell-based module. (a) module circuit display, (b) a complete set of modules, and (c) module test with a mini motor.

CONCLUSIONS

Supercapacitors based on nanocomposite electrodes were successfully fabricated in coin cells, pouch cells, and coin cell-based modules. PVDF and ethanol are binders and solvents in a coin cell supercapacitor, while the pouch cell electrodes use CMC and water. According to electrochemical characterization, the laboratory-fabricated supercapacitor has similar characteristics to commercial devices. Furthermore, the GCD coin cell has a coulombic efficiency of 100% and capacitance retention of 97% after 1000 cycles.

ACKNOWLEDGEMENT

The author is grateful to the Ministry of Finance of the Republic of Indonesia for providing funds for this research through the BPDPKS (Badan Pengelola Dana Perkebunan Kelapa Sawit) Research Grant 2020 (No. PRJ/21/DPKS/2020).

REFERENCES

Allebrod, F., Chatzichristodoulou, C., Mollerup, P. L., and Mogensen, M. B., 2012. "Electrical conductivity measurements of aqueous and immobilized potassium hydroxide," *Int. J. Hydrog. Energy,* 37, 16505-16414.

Antonietti, M., Chen, X. D., Yan, R. Y., and Oschatz, M., 2018. "Storing electricity as chemical energy: beyond traditional electrochemistry and double-layer compression," *Energy Environ. Sci*., 11, 3069–30

Augustyn, V., Simon, P., and Dunn, B., 2014. "Pseudocapacitive oxide materials for high-rate electrochemical energy storage," *Energy Environ. Sci*., 7, 1597–1614.

Azaïs, P., Duclaux, L., Florian, P., Massiot, D., and Lillo-Rodenas, M. A., 2017. "Causes of supercapacitors aging in an organic electrolyte," *J. Power Sources,* 171, 1046–1053.

Balducci A., Belanger, D., Brousse, T., Long, J. W., and W. Sugimoto., 2017. "A guideline for reporting performance metrics with electrochemical capacitors: from electrode materials to full devices," *J. Electrochem. Soc.*, 164 (7), A1487-A1488.

Beguin, F. and Frackowiak, E., 2013. Supercapacitors: materials, systems, and applications, Wiley-VCH Verlag GmbH & Co. KgaA, Weinheim, Germany

Bonaccorso, F., Colombo, L., Yu, G., Stoller, M., Tozzini, V., Ferrari, A. C., Ruoff, R.S., and Pellegrini., 2015. "Graphene, related two-dimensional crystals, and hybrid systems for energy conversion and storage," *Science*, 347 (*6217*), 10.

Cheng, F., Yang, X., Zhang, S., and Lu., 2020. "Boosting the supercapacitor performances of activated carbon with carbon nanomaterials," *J. Power Sources*, 450, 227678.

Cheng, Q., Tang, J., Ma, J., Zhang, H., Shinyaa, N., dan Qin, L. Q., 2011. "*Graphene* dan carbon nanotube composite electrodes for supercapacitors with ultra-high energy density," *Phys. Chem. Chem. Phys*., 13, 17615–17624.

Chernysh, O., Khomenko, V., Makyeyeva, I., and Barsukov, V., 2019. "Effect of binder's solvent on the electrochemical performance of electrodes for lithium-ion batteries and supercapacitors," *Mater. Today: Proc.,* 6, 42–47.

Giurlani, W., Sergi, L., Crestini, E., Calisi, N., Poli, F., Soavi, F., and Innocenti, M., 2022. "Electrochemical stability of steel, Ti, and Cu current collectors in water-in-salt electrolyte for green batteries and supercapacitors," *J. of Solid State Electrochem*., 26, 85–95.

Marshall, J. E., Zhenova, A., Roberts, S., Petchey, Zhu, P., Dancer, C. E. J., McElroy, C. R, Emma Kendrick, E., and Goodship, V., 2021. "On the solubility and stability of polyvinylidene fluoride," *Polymers*, 13, 1354.

Kumar, V. B., Borenstein, A., Markovsky, B., Aurbach, D., Gedanken, A., Talianker, M., and Porat, Z, 2016. "Activated carbon modified with carbon nanodots as novel

electrode material for supercapacitors," *J. Phys. Chem. C*, 120, 13406−13413.

Liang, K., Wang, W., Yu, Y., Liu, L., Haijun, L., Zhang, Y., and Chen, A., 2019. "Synthesis of nitrogen-doped mesoporous carbon for high-performance supercapacitors," *New J. Chem.,* 43, 2776-2782.

Liu, J., Deng, Y., Li, X., dan Wang, L., 2016. "Promising nitrogen-rich porous carbons derived from one-step calcium chloride activation of biomass-based waste for high-performance supercapacitors," *ACS Sustain. Chem. Eng*., 4, 177-187.

Liu, C. and Liu, L., 2017. "Optimal design of Li-ion batteries through multi-physics modeling and multi-objective optimization," *J. Electrochem. Soc*, 164 (11), E3254-E3264.

Liu, Z., Zhu, Z., Dai, J., and Yan, Y., 2018. "Waste biomass based-activated carbons derived from soybean pods as electrode materials for high-performance supercapacitors," *Chemistry Select.,* 3, 5726 – 5732.

Lukatskaya, M. R., Dunn, B., and Gogotsi, Y., 2016. "Multidimensional materials and device architectures for future hybrid energy storage," *Nat. Commun*., 7, 12647–12659.

Pal, B., Yang, S., Ramesh, S., Thangadurai, V., and Jose, R., 2019. "Electrolyte selection for supercapacitive devices: a critical review," *Nanoscale Adv.,* 1, 3807–3835.

Scibioh, M. A. and Viswanathan, B., 2020a. Materials for Supercapacitor Applications. Elsevier, New York, USA.

Scibioh, M. A. and Viswanathan, B., 2020b. *Materials for Supercapacitor Applications*. Elsevier, New York, USA

Shao, H., Wu, Y. C., Lin, Z., Taberna, P. L., and Simon, P., 2020. "Nanoporous carbon for electrochemical capacitive energy storage," *Chem. Soc. Rev*., 49, 3005–3039.

Singh A. P., Karandikar, P. B., and Tiwari, N. K., 2015. "Effect of electrode shape on the parameters of the supercapacitor," *IEEE,* 2015, 669–673.

Sinha, P., Banerjee, S., and Kar, K. K., 2020. Characteristics of Activated Carbon. Vol 300, *Kar K. K., ed.,* Springer, Cambridge, United Kingdom.

Simon, P. and Gogotsi, Y., 2020. "Perspectives for electrochemical capacitors and related devices," *Nat. Matter*., 19, 1151-1161.

Stephane, K. D., Gupta, M., Kumar, A., Sharma, V., Pandit, S., Bocchetta, P., and Kumar, Y., 2021. "The effect of activated carbon materials modifications on the capacitive performance: surface, microstructure, and wettability," J. *Compos. Sci.,* 5, 66.

Tanwilaisiri, A., Xu, Y., Zhang, R., Harrison, D., Fyson, J., and Areir, M., 2018. "Design and fabrication of modular supercapacitors using 3D printing", *J. Energy Storage,* 16, 1-7.

Trask, S. E., Kubal, J. J., Bettge, M., Bryant, J., Polzin, B. J., Zhu, Y., Danrew N., Jansen, A. N., and Abraham, D. P., 2014. "From coin cel*l*s to 400 mAh *pouch cell*s: Enhancing performance of high-capacity lithium-ion cells via modifications in electrode constitution dan fabrication", *J. of Power Sources,* 259, 233-244.

Wang, Y., Song, Y., and Xia, Y., 2016. " Electrochemical capacitors: mechanism, materials, systems, characterization and applications," *Chem. Soc. Rev*., 45, 5925–5950

Wang, F., Wu X, Yuan, X., Liu, Z., Zhang, Y., Fu, L., Zhu, Y., Zhou, Q., Wu, Y., and Huang, W., 2017. "Latest advances in supercapacitors: from new electrode materials to novel device designs," *Chem. Soc. Rev.,* 46, 6816–6854.

Wulandari, N.N., Rustamaji, H., Fibarzy, W.U., Prakoso, T., Rizkiana, J., Devianto, H., Widiatmoko, P., and Nurdin, I., 2020. "Production of activated carbon from palm empty fruit bunch as supercapacitor electrode material." *IOP Conf. Series: Mater. Sci. Eng.,* 1143(1), 012004.

Xu Z., Li, Y., Li, D., Wang, D., Zhao, J., Wang, Z., Banis, M. N., Hu, Y., and Zhang, H., 2018. "N-enriched multilayered porous carbon derived from natural casings for high-performance supercapacitors," *Appl. Surf. Sci.*, 444, 661–667.

Yang, W., Li, Y., and Feng, Y., 2018. "High electrochemical performance from oxygen functional groups containing porous activated carbon electrode of supercapacitors," *Materials*, 11, 2455.

Yang, H., Kannappan, S., Pandian, A. S., Jang, J. H., Lee, Y. S., and Lu, W., 2017. "Rapidly annealed nanoporous graphene materials for electrochemical energy storage," *J. Mater. Chem. A,* 5, 23720–23726.

Zhang, F., Zhang, T., Yang, X., Zhang, L., Leng, K., Huang, Y., and Chen, Y., 2013. "High-performance supercapacitor-battery hybrid energy storage device based on graphene-enhanced electrode materials with ultrahigh energy density," *Energy Environ. Sci.,* 6, 1623-1632.

Zheng, Z. and Gao, Q., 2011. "Hierarchical porous carbons prepared by an easy one-step carbonization and activation of phenol-formaldehyde resins with high performance for supercapacitors," *J. Power Sources* 196, 1615–1619.

Zhong, C., Deng, Y, Hu, W., Jinli Qiao, J., Zhang, L., and Zhang, J., 2015. "A review of electrolyte materials and compositions for electrochemical supercapacitors," *Chem. Soc. Rev.*, 44, 7484-7.